Radio Observations of the Supernova Remnant Candidate G312.5-3.0

Stephen R. Kane[1] and Alan E. Vaughan[2]

[1]*School of Physics & Astronomy, University of St Andrews, North Haugh, St Andrews, Fife KY16 9SS, Scotland*
[2]*Department of Physics, Macquarie University, Sydney, NSW 2109, Australia*

24 November 2018

ABSTRACT

The radio images from the Parkes-MIT-NRAO (PMN) Southern Sky Survey at 4850 MHz have revealed a number of previously unknown radio sources. One such source, G312.5-3.0 (PMN J1421-6415), has been observed using the multi-frequency capabilities of the Australia Telescope Compact Array (ATCA) at frequencies of 1380 MHz and 2378 MHz. Further observations of the source were made using the Molonglo Observatory Synthesis Telescope (MOST) at a frequency of 843 MHz. The source has an angular size of 18′ and has a distinct shell structure. We present the reduced multi-frequency observations of this source and provide a brief argument for its possible identification as a supernova remnant.

Key words: ISM: HII regions – supernova remnants

1 INTRODUCTION

Extensive radio surveys of the sky began in the 1950s when the number of identified sources was not sufficient to conduct significant statistical studies. The large-area continuum radio surveys have become the foundation for all other radio astronomy tests since they provide the necessary radio source catalogues and the location of objects with which astronomers can calibrate their instruments.

The Parkes-MIT-NRAO (PMN) survey of the southern sky was undertaken as a collaboration between the Parkes Radio Observatory of the Australia Telescope National Facility (ATNF), the Massachusetts Institute of Technology (MIT), and the National Radio Astronomy Observatory (NRAO) (Griffith & Wright 1993). The primary aim of the project was to survey the whole southern sky at a frequency of 4850 MHz in order to provide a more extensive, high-quality catalogue of radio sources for the Southern Hemisphere. The secondary aim was to use this survey to complement the results obtained from the Northern Hemisphere 4850 MHz survey performed by Condon, Broderick, & Seielstad (1989) which was made using the NRAO 91 m telescope (Wright et al. 1994). Previously, the only large-area, high-frequency radio survey in the same area was the 2700 MHz survey of Bolton and his collaborators which contains around 8200 sources (Griffith et al. 1991).

The Southern Survey ($-87.5° < \delta < -37°$) and the Tropical Survey ($-29° < \delta < -9.5°$) increased the number of known radio sources in the Southern and Tropical zones by a factor of about 5 over those known previously from the Parkes 2700 MHz and Molonglo 408 MHz surveys

(Griffith & Wright 1993). The catalogue of radio sources discovered in the Southern Survey contains 23,277 sources. However, it is important to realise that the PMN surveys primarily detected point sources and the reduction process was optimised for such objects. This resulted in the exclusion of many extended objects from the survey with the exception of stronger sources which had a sufficiently high signal-to-noise ratio (Wright et al. 1994).

It was from an image of the PMN survey that the chosen object of study was discovered. The object is at right ascension 14^h20^m and declination $-64.2°$ (Galactic longitude $312.5°$ and latitude $-3°$) and has an approximate diameter of 18′. The object is shown towards the centre of Figure 1 which is a map taken from the PMN survey. The circular appearance of the object suggests it may be a supernova remnant (SNR) although it does not currently appear in SNR catalogues. The source has also been noted as a SNR candidate by Duncan et al. (1997). The object seems to have no optically visible counterpart and no counterpart has been found in current ROSAT data. Shown in Figure 2 is an IRAS 12 micron image from the same region of sky as the object (McGlynn et al. 1996). This indicates that the object may have a strong counterpart in the infra-red, although dust in the local environment makes further conclusions based on the IR data difficult.

2 OBSERVATIONS AND DATA REDUCTION

The extended source was observed in January, 1995 using the mosaic capabilities of the Australia Telescope Compact
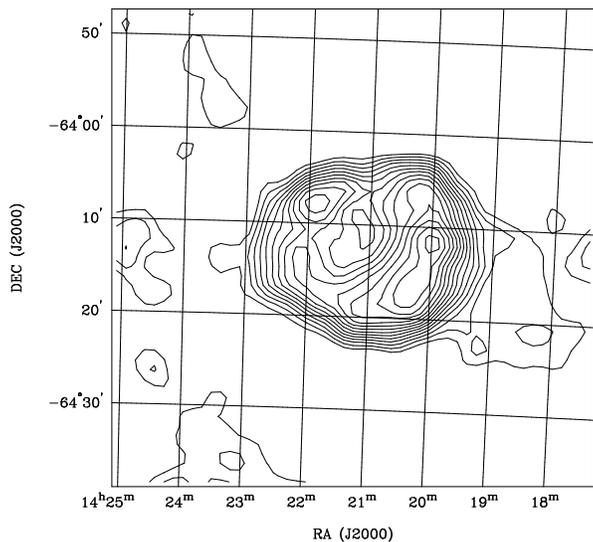
Figure 1. A contour map from the PMN survey showing the object of interest. The contour levels start at 10 mJy/Beam and increase in steps of 10 mJy/Beam.
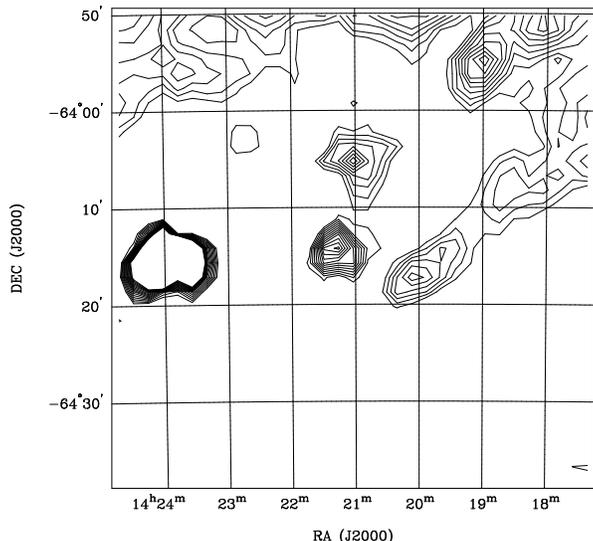
Figure 2. A contour map from the IRAS 12 micron survey showing the same region of sky. The contour levels start at 380 mJy/□′ and increase in steps of 8 mJy/□′.

Array (ATCA). The observation used a 19 pointing centre mosaic in a hexagonal grid with the pointing centres set 12′ apart from each other. The radio sources 1934-638 and 0823-500 were used as the primary calibrators and 1549-790 was used as the secondary calibrator. The object was observed at frequencies of 1380 MHz and 2378 MHz which, along with a baseline of 375 m, were chosen to approximately match the resolution of the PMN survey at 4850 MHz. Each band had a width of 128 MHz divided into 32 channels.

The allocated observing time began at 10:30 UT, January 17 and extended through to 2:30 UT, January 18 and allowed an approximate 12 hour synthesis observation of the source. The observations are summarised in Table 1.

The reduction of the ATCA data was performed using the software package Miriad which was developed

Table 1. ATCA observations of G312.5-3.0

Parameter	1380 MHz	2378 MHz
Configuration (m)	375	375
Bandwidth (MHz)	128	128
Integration time (min)	720	720
Beam Size (FWHM)	$115.99'' \times 128.83''$	$67.31'' \times 74.76''$
rms noise (mJy beam^{-1})	0.029	0.040
Diameter	20′	20′

by the Berkeley Illinois Maryland Association (BIMA) and then later adapted to the needs of the ATNF (Sault, Teuben, & Wright 1995). The software package contains tasks designed to reduce data from mosaic observations. The results from these reductions are presented in the next section.

Further observations of the source were made using the Molonglo Observatory Synthesis Telescope (MOST) at a frequency of 843 MHz which served to complement the data obtained from the Compact Array. The observation was carried out in September, 1995 and the observed field has an area of $70' \times 70'$. The phase gradient of the MOST, together with the tilting of the east-west arm about its long axis, provides the equivalent of an alt-alt mounting which has full uv-coverage for declinations south of $-30°$ (Mills 1981, 1985).

3   RESULTS AND DISCUSSION

Radio images of the source have been produced from the observations. The images shown in Figures 3, 4, and 5 are the contour maps of the extended source at frequencies of 843 MHz, 1380 MHz, and 2378 MHz respectively. These images may be used as a first step to determine some of the astrophysical properties of the source in an attempt to discover its nature and the emission processes which are occurring. This information assists in constraining the identity of the source as either a H I region, a H II region, a SNR, or a planetary nebula.

3.1   Morphology

At each frequency, the object appears to be faint in the middle with a ring structure around the edge. This indicates that the object is likely to be a spherical shell, which is a structure typical of planetary nebulae and shell remnants produced by Type I supernovae (Milne 1979; Milne et al. 1985; Mallik 1991; Aller 1994). The symmetry of the images also suggests that the extended region originated at a central location whereas H I and H II regions tend to be amorphous clouds with no axis of symmetry. At the side of smaller right ascension, the intensity of the object appears to be higher, indicating that this region may have more mass or is more dense (or both). This is probably due to interactions with the interstellar medium. The observed shell structure suggests that the source is optically thin at the observed frequencies.

For an optically thin source, the equation of radiative transfer can be approximated by

$$I_\nu = S_\nu \tau_\nu \tag{1}$$
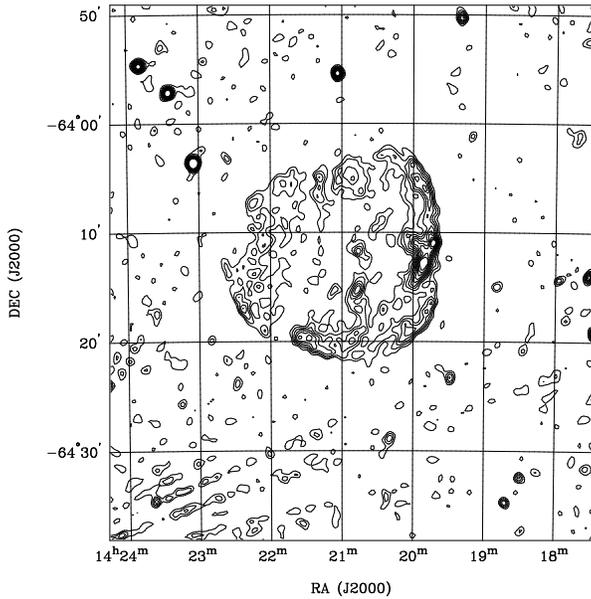
Figure 3. A contour map of the extended source at 843 MHz. The contour levels start at 2 mJy/Beam and increase in steps of 2 mJy/Beam. Structure in the image due to a nearby strong source just outside the field is also visible.
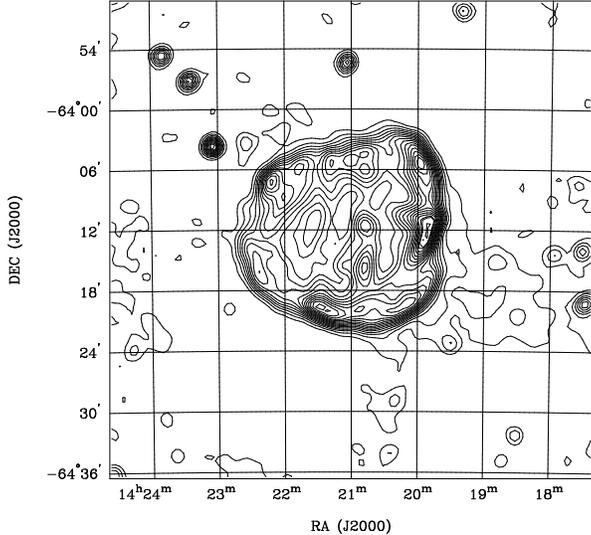
Figure 4. A contour map of the extended source at 1380 MHz. The contour levels start at 2 mJy/Beam and increase in steps of 2 mJy/Beam.

where the source function S_ν is defined as $S_\nu \equiv j_\nu/\alpha_\nu$ and where α_ν and j_ν are the absorption and emission coefficients of the medium respectively.

Assuming the source function to be constant throughout the source, equation (1) may be expressed as a ratio

$$\frac{I_1}{I_2} = \frac{\tau_1}{\tau_2}$$

where the subscripts refer to two paths through the source. By measuring the flux density at the edge and at the middle of the object, this ratio was estimated to be $I_1/I_2 = 2.27$.
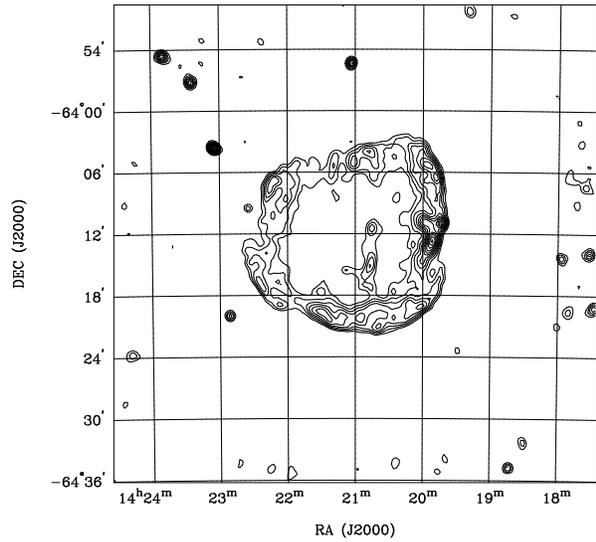
Figure 5. A contour map of the extended source at 2378 MHz. The contour levels start at 2 mJy/Beam and increase in steps of 2 mJy/Beam.

Table 2. Total flux density at each frequency.

Frequency (MHz)	Flux Density (Jy)
843	1.1 ± 0.2
1380	3.0 ± 0.6
2378	1.3 ± 0.3
4850	1.2 ± 0.2

The absorption coefficient will be constant throughout the source so from the definition of optical depth

$$\frac{\tau_1}{\tau_2} = \frac{s_1}{s_2}$$

where s is the path length. By estimating the width of the shell to be approximately $3'$, the path lengths through the middle and through the edge were calculated. The ratio was then estimated to be $s_1/s_2 = 2.23$. The near equality of the two ratios confirms that the source is optically thin, based on the assumption of constant absorption within the source.

3.2 Flux Densities

The estimated total flux density at each frequency is shown in Table 2. The errors associated with the flux density measurements at each frequency are mainly due to (unknown) losses of flux density in the lower spatial frequencies for each of the images. Due to the low-pass filter applied to the PMN data during the reduction process, it should be noted that the flux given at 4850 MHz is likely a lower limit to the flux at this frequency.

The response of the ATCA interferometer to the shortest spatial frequencies is different from that of the Parkes and Molonglo radio telescopes. Hence, it is difficult to make a direct comparison of the total flux densities.

3.3 Polarisation

Synchrotron radiation from electrons in a uniform magnetic field is highly directional and so should be linearly polarised

(Moffett & Reynolds 1994a). Ideally, the orientation of the magnetic field may be determined from the polarisation position angle. This assumes that the magnetic field is an ordered field in a vacuum.

Relatively young SNRs are known to have quite large depolarisation effects due to disorder in the magnetic field in the source itself (Moffett & Reynolds 1994a,b). Polarisation images of the Q and U Stokes parameters were obtained which showed that there is no significant polarisation in the extended source. This lack of polarisation is confirmed by Duncan et al. (1997), who reports no apparent polarisation at 2.4 GHz.

3.4   Distance and Size

Distances to SNRs can occasionally be obtained indirectly either from measuring optical velocities and proper motions or from positional coincidences with H I and H II regions, OB associations, or pulsars. However, the simple (but disputed) method of using the radio surface brightness-to-diameter relationship $(\Sigma - D)$ (Case & Bhattacharya 1996, 1998) is adopted here to obtain a distance estimate for the observed source, assuming that it is a SNR.

The radio surface brightness is defined as

$$\Sigma_\nu \equiv 1.505 \times 10^{-19} \frac{S_\nu}{\theta^2} \, \text{W m}^{-2} \, \text{Hz}^{-1} \, \text{sr}^{-1} \tag{2}$$

where S_ν is in Janskys and θ is in arcminutes. The $\Sigma - D$ relation for Galactic shell remnants derived by Case & Bhattacharya (1998) is given by

$$\begin{aligned}
\Sigma_{1\,\text{GHz}} \quad = \quad & 2.07^{+3.10}_{-1.24} \times 10^{-17} \\
& \times D^{(-2.38 \pm 0.26)} \, \text{W m}^{-2} \, \text{Hz}^{-1} \, \text{sr}^{-1} \tag{3}
\end{aligned}$$

where the diameter D is in parsecs. The distance follows directly.

In the case of the observed object, the flux density S_ν at 1 GHz was estimated (assuming the spectrum shown in Figure 6 peaks before 1 GHz) to be 3.5 ± 0.7 Jy. From equation (2), the radio surface brightness was estimated to be $\Sigma_{1\,\text{GHz}} = 1.626 \times 10^{-21} \, \text{W m}^{-2} \, \text{Hz}^{-1} \, \text{sr}^{-1}$. The diameter of the object was then estimated from equation (3) to be $D \approx 53$ pc. This leads to an estimate of the distance to the source of ≈ 10 kpc.

The uncertainty in these calculations are subject to the errors inherent in the assumptions with the $\Sigma - D$ relation. These are the assumptions that all shell remnants have the same radio luminosity dependence on linear diameter, have the same supernova explosion mechanism and energy, and are evolving into identical environments (Case & Bhattacharya 1998). It has been concluded by Green (1984) that the $\Sigma - D$ relation is severely limited and that the distance determinations may have a factor of 3 error. However, by using known distances to SNRs as distance "calibrators", Case & Bhattacharya (1998) find the error in their derived $\Sigma - D$ relation to be $\sim 40\%$.

4   CONCLUSIONS

Mosaic observations of an extended source from the PMN survey were carried out using the ATCA in early 1995 at frequencies of 1380 MHz and 2378 MHz. To complement these data, further observations of the source were obtained from the MOST at a frequency 843 MHz.

The morphology of the extended object shows a distinct shell structure which is optically thin. This is common to both SNRs and planetary nebulae. In the case of a SNR, a shell structure would indicate that the remnant was possibly produced by a Type I supernova resulting from the collapse of a white dwarf star. Interactions with the interstellar medium may have produced variations in the spherical nature of the remnant's structure.

If the source is a SNR, the lack of significant polarisation suggests that the intervening magnetic fields are disordered or that the SNR candidate is at a large distance.

An estimate of the source's distance was made using the $\Sigma - D$ relation for Galactic shell remnants. This yielded a diameter of ≈ 53 pc and a distance of ≈ 10 kpc. These results are consistent with the known parameters of SNRs and that the apparent lack of linear polarisation is likely due to the large distance. The distance estimate is of course dependant on the source being a SNR.

Since interferometers do not respond to the shortest spatial frequencies, it is difficult to compare total flux densities from ATCA observations with those from the Parkes Radio Telescope. The 1.38 GHz and 2.38 GHz results may be improved by using the Parkes telescope which contains the lower spacings. Additional spectral information may be obtained from further observations using the ATCA and the Parkes telescope at X-Band (8000–9200 MHz). It would also be useful to obtain X-ray spectra of the source to gain an estimate of the shock velocity and thus determine the age and expansion rate of the SNR candidate.

REFERENCES

Aller, L.H., 1994, ApJ, 432, 427
Case, G.L. & Bhattacharya, D., 1996, A&AS, 120, 437
Case, G.L. & Bhattacharya, D., 1998, ApJ, 504, 761
Condon, J.J., Broderick, & J.J., Seielstad, G.A., 1993, AJ, 97, 1064
Duncan, A.R., Stewart, R.T., Haynes, R.F., & Jones, K.L., 1997, MNRAS, 287, 722
Green, D.A., 1984, MNRAS, 209, 449
Griffith, M.R. & Wright, A.E., 1993, AJ, 105, 1666
Griffith, M., et al., 1991, PASA, 9, 243
Mallik, D.C.V., 1991, PASA, 9, 15
McGlynn, T., Scollick, K., White, N., 1996, in Proc. IAU Symp. 179, New Horizons from Multi-Wavelength Sky Surveys, ed. B.J. McLean et al., p.465
Mills, B.Y., 1981, PASA, 4, 156
Mills, B.Y., 1985, PASA, 6, 72
Milne, D.K., 1979, PASA, 3, 341

Milne, D.K., Caswell, J.L., Haynes, R.F., Kesteven, M.J.,
  Wellington, K.J., Roger, R.S., & Bunton, J.D., 1985,
  PASA, 6, 78
Moffett, D.A. & Reynolds, S.P., 1994, ApJ, 425, 668
Moffett, D.A. & Reynolds, S.P., 1994, ApJ, 437, 705
Sault, R.J., Teuben T.J., Wright, M.C.H., 1995, in Shaw
  R., Payne H.E., Hayes, J.J.E., eds, ASP Conf. Ser. Vol.
  77, Astronomical Data Analysis Software and Systems IV.
  Astron. Soc. Pac., San Francisco, p. 433
Wright, A.E., Griffith, M.R., Burke, B.F., & Ekers, R.D.,
  1994, ApJS, 91, 111